International Journal of Industrial Chemistry (IJIC)
a SpringerOpen Journal

RESEARCH Open Access

Low-temperature preparation and physical characterization of doped $BaCeO_3$ nanoparticles by chemical precipitation

Joseph Sundar Singh Jasmine Ketzial, Devi Radhika and Arputharaj Samson Nesaraj*

Abstract

Background: In this work, the nanoparticles of pure $BaCe_{1-x}M_xO_{3-\delta}$ (where M = Gd or Sm and x = 0, 0.10, or 0.20) were synthesized by the simple chemical precipitation method. The prepared materials were calcined at 300°C, 450°C, and 600°C for 2 h each to obtain phase-pure compounds. The samples were characterized by thermogravimetry/differential thermal analysis (TGA/DTA), X-ray diffraction (XRD), energy-dispersive X-ray spectroscopy (EDAX) analysis, Fourier transform infrared (FTIR), particle size analysis, and scanning electron microscopy.

Results: TGA/DTA results have shown that phase-pure $BaCeO_3$ materials can be formed only above 500°C. The crystalline structure of parent and doped $BaCeO_3$ was found to be orthorhombic. EDAX analysis has shown the atomic percentage of elements present in the Gd- and Sm-doped $BaCeO_3$ samples. FTIR studies have shown the presence of Ce-O in doped $BaCeO_3$ nanoparticles.

Conclusions: Doped $BaCeO_3$ may be used as an electrolyte for solid oxide fuel cell applications.

Keywords: Gd/Sm-doped $BaCeO_3$, Nanosized powder, Chemical precipitation, Physical characterization

Background

Complex cerium oxides with perovskite-related structures are promising ceramic materials for application in hydrogen sensors, electro-catalytic reactors for hydrogen separation, and also as electrolytes in solid oxide fuel cells operating on hydrocarbon fuels. $BaCe_{1-x}M_xO_{3-\delta}$ (M = trivalent ion such as Y, Yb, Nd, Gd, Sm, and so on) has been studied as a high proton conducting oxide operated at 400°C to 600°C, which is expected as an electrolyte of solid oxide fuel cells [1-3], hydrogen separation membranes, hydrogen gas sensors [4,5], and so on. Recently, these materials were also found to be of broad interest as catalysts for oxidation reactions because of their ability to conduct oxygen and to support significant variations in oxygen contents [6]. As well known, in the next generation of energy devices such as solid oxide fuel cells (SOFC), there is considerable emphasis on moving to lower temperature of operation. One of the important problems in this direction will be addressed to find suitable materials that operate well at lower temperatures. Good progress can be achieved using perovskites such as doped $BaCeO_3$. For this reason, $BaCeO_3$ phases doped by different dopants seem to be perspective materials for future application. These materials are usually formed by a conventional ceramic process consisting of calcining mixtures of the respective oxides and carbonates at temperatures >1,200°C followed by sintering of the powder compacts at temperatures of 1,400°C to 1,600°C [7]. The solid-state reaction is a diffusion-controlled process which requires intimacy of reacting species and a uniform distribution of each species to obtain a completely reacted and uniform product. Since the starting materials generally have a large particle size, this approach frequently needs repeated mixing and extended heating at high temperature in order to generate a homogeneous and single-phase material [8]. The mechanical mixing process will very likely introduce contaminants from abrasive materials [9]. Moreover, prolonged calcination promotes crystallite growth, which is undesirable in the fabrication of dense fine-grained ceramics which undoubtedly possess better electrical properties. In order to overcome all these disadvantages, wet chemical routes like coprecipitation of metal ions may be a promising alternative. The principal advantages of starting

* Correspondence: drsamson@karunya.edu
Department of Chemistry, Karunya University (Karunya Institute of Technology and Sciences), Coimbatore, Tamil Nadu 641 114, India

Table 1 Amount of precursor materials (dissolved in 100 ml of water) used to prepare $BaCe_{1-x}Gd_x/Sm_xO_{3-\delta}$ nanoparticles

Sample	Molarity of $(Ba(NO_3)_2$/amount (g)	Molarity of Ce $(NO_3)_3$/amount (g)	Molarity of $Gd(NO_3)_3$/ amount (g)	Molarity of $Sm(NO_3)_3$/ amount (g)	Molarity of NaOH/amount (g)
$BaCeO_3$	0.05:1.306	0.05:2.171	-	-	0.3:1.2
$BaCe_{0.9}Gd_{0.1}O_{3-\delta}$	0.25:6.5335	0.225:9.7625	0.025:0.4531 g of Gd_2O_3 dissolved in HNO_3/water	-	1.475:5.9
$BaCe_{0.8}Sm_{0.2}O_{3-\delta}$	0.25:6.5335	0.2:6.5228	-	0.05:0.8718 g of Sm_2O_3 dissolved in HNO_3/water	1.45:5.8

from a solution are better homogeneity and improved reactivity. The necessary solid-state reactions proceed more rapidly and at lower temperatures. As a consequence, the desired product can be obtained with a smaller particle size and greater reactivity. To date, only a few wet chemical processes were attempted to prepare such materials. Based on the fact that doped $BaCeO_3$ phases have good perspective as proton conductors, we decided to prepare $BaCeO_3$ (BC) with compositions such as $BaCe_{0.9}Gd_{0.1}O_{3-\delta}$ and $BaCe_{0.8}Sm_{0.2}O_{3-\delta}$ systems (abbreviated as BCGO and BCSO) and characterize them. In this research work, we focus our attention on the synthesis of the above ceramic materials by the chemical precipitation process. The main purpose of this work is to prepare Gd/Sm-doped $BaCeO_3$

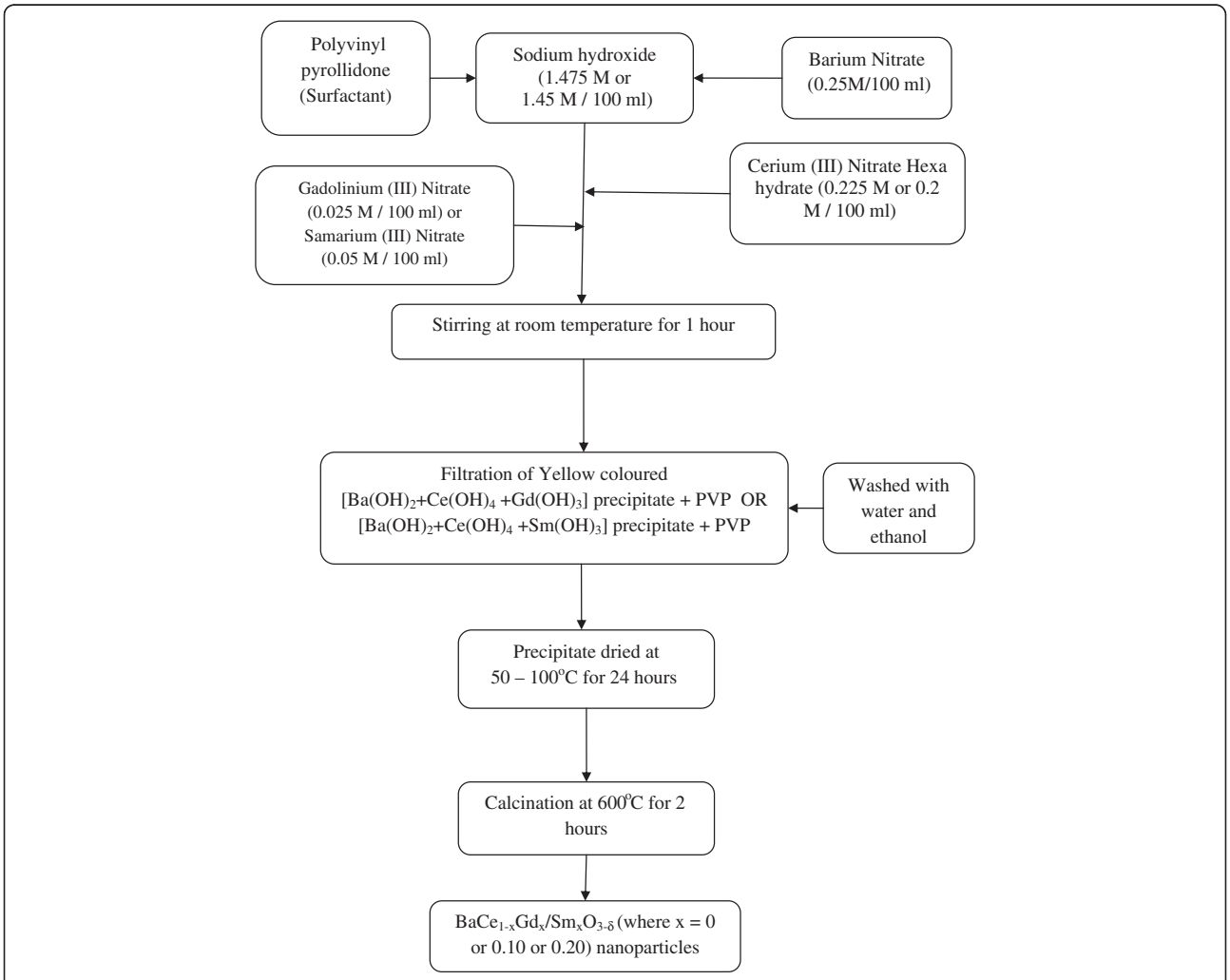

Figure 1 The synthesis of $BaCe_{1-x}Gd_x/Sm_xO_{3-\delta}$ (where x = 0, 0.10, or 0.20) nanoparticles by chemical precipitation.

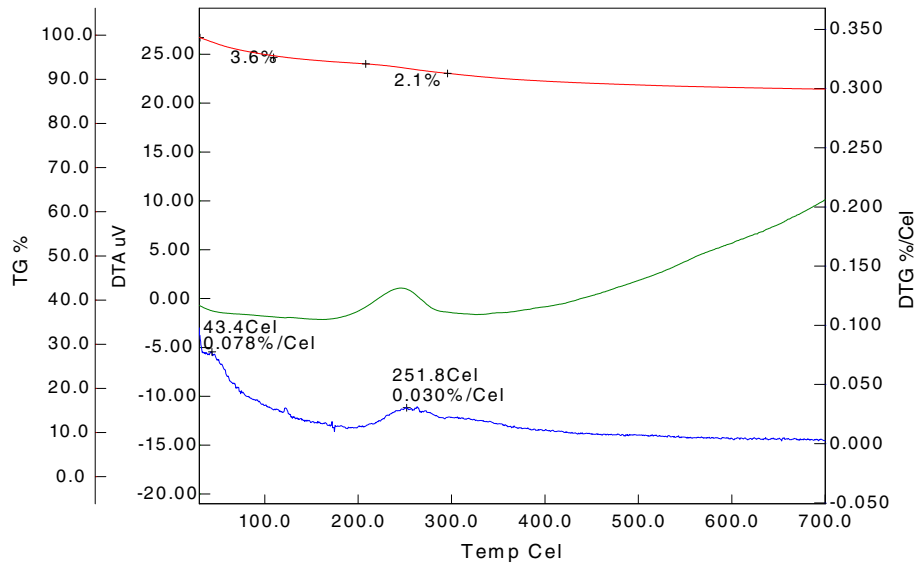

Figure 2 TGA/DTA spectrum obtained with the precursor material ($Ba(OH)_2$ + $Ce(OH)_4$ + $Gd(OH)_3$ + PVP).

by the chemical precipitation method in the presence of sodium hydroxide (precipitant) and polyvinyl pyrrolidone (PVP, surfactant) and to study the basic structural and particulate properties of the samples.

Methods

Preparation of $BaCe_{1-x}Gd_x/Sm_xO_{3-\delta}$ (where x = 0, 0.10, or 0.20) nanoparticles by chemical precipitation process

In the typical experiment, the aqueous solution containing a known concentration of barium nitrate, cerium nitrate, and gadolinium nitrate/samarium nitrate (as basic materials) and sodium hydroxide (as precipitator material) was prepared in distilled water. Gadolinium nitrate/samarium nitrate was prepared by dissolving the required quantity of Gd_2O_3/Sm_2O_3 in HNO_3. Initially, the precipitating solution (sodium hydroxide) was mixed with 2 ml of 10% PVP (as surfactant material). To this mixture, $Ba(NO_3)_2$, $Ce(NO_3)_3$, and $Gd(NO_3)_3/Sm(NO_3)_3$ solutions were consequently added one by one dropwise. They were mixed perfectly by a magnetic stirring apparatus

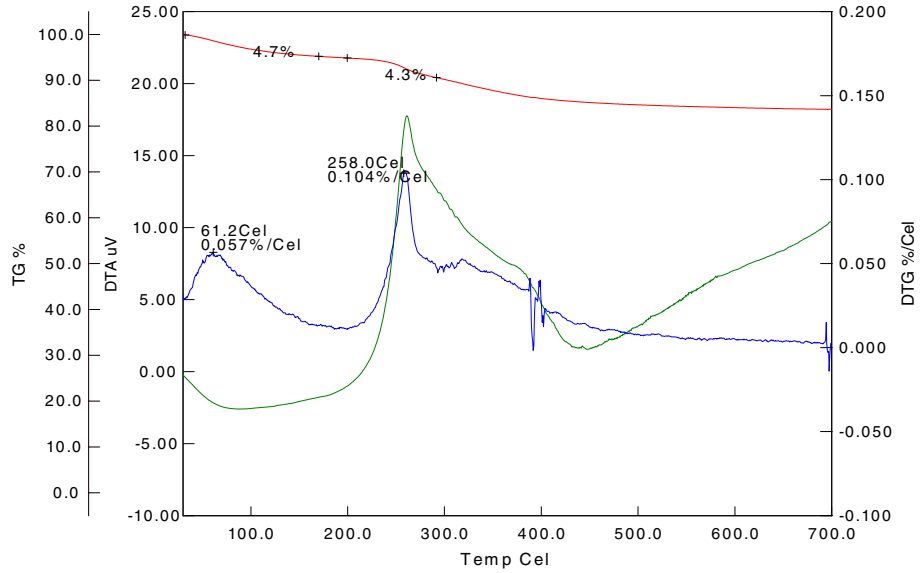

Figure 3 TGA/DTA spectrum obtained with the precursor material ($Ba(OH)_2$ + $Ce(OH)_4$ + $Sm(OH)_3$ + PVP).

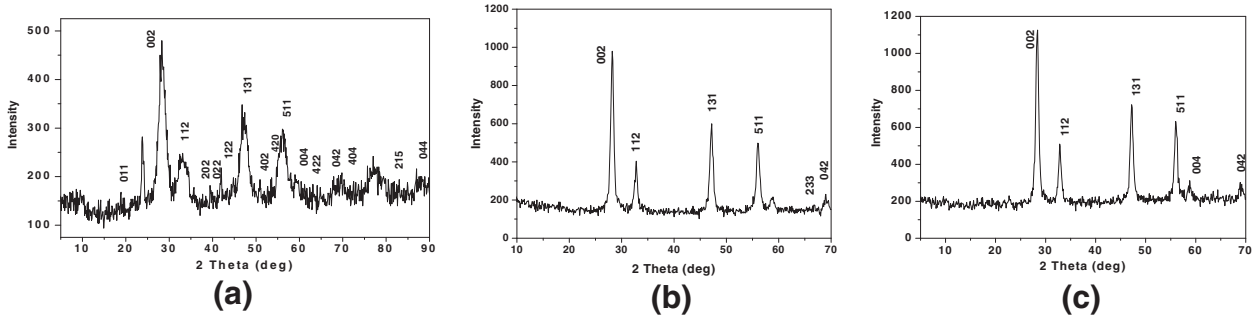

Figure 4 XRD patterns. Obtained with calcined (**a**) BC, (**b**) BCGO, and (**c**) BCSO powders prepared by chemical precipitation method.

(1,000 rpm) at room temperature for 1 h. The pH was maintained at greater than 9 throughout the experiment by the addition of alkali. The resultant yellow-colored precipitate ($(Ba(OH)_2 + Ce(OH)_4 + Gd(OH)_3$ with PVP) or ($(Ba(OH)_2 + Ce(OH)_4 + Gd(OH)_3$ with PVP)) was filtered and then washed with deionized water and ethanol five to ten times. The product was dried at 50°C to 100°C for 24 h. The resultant material was calcined at 300°C, 450°C, and 600°C for 2 h each. During calcination, the surfactant was removed, and phase-pure, yellow-colored $BaCe_{1-x}Gd_xO_{3-\delta}$ or $BaCe_{1-x}Sm_xO_{3-\delta}$ was formed. To study the crystallographic parameters of undoped $BaCeO_3$, parent $BaCeO_3$ was also prepared using the same process without the addition of $Gd(NO_3)_3/Sm(NO_3)_3$. The amount of precursor materials used for the preparation of $BaCe_{1-x}Gd_x/Sm_xO_{3-\delta}$ (where x = 0, 0.10, or 0.20) nanoparticles is indicated in Table 1. Figure 1 shows a schematic of the synthesis of $BaCe_{1-x}Gd_x/Sm_xO_{3-\delta}$ (where x = 0, 0.10, or 0.20) by chemical precipitation. The main reactions involved in the preparation of parent $BaCeO_3$, $BaCe_{0.9}Gd_{0.1}O_{3-\delta}$, and $BaCe_{0.8}Sm_{0.2}O_{3-\delta}$ during the experimental procedure can be written briefly as follows:

Reaction mechanism involved in the preparation of parent $BaCeO_3$:

Table 2 XRD data obtained with parent BC powder

Standard XRD data for orthorhombic $BaCeO_3$ powder (JCPDS no. 22–74)			Powder XRD data for $BaCe_{0.9}Gd_{0.1}O_{2-\delta}$					
d values (Å)	*hkl* values	I/I_o	d_{obs} (Å)	d_{cal} (Å)	*hkl* values	2θ values (obs)	2θ values (cal)	I/I_o (obs)
4.41	011	2	4.7014	4.4094	011	18.8750	20.1379	4
3.12	002	100	3.1462	3.1547	002	28.3670	28.2886	100
2.659	112	2	2.7043	2.6723	112	33.1250	33.5339	32
2.545	202	2	2.5150	2.5529	202	35.7000	35.1523	5
2.202	022	40	2.2676	2.2047	022	39.7500	40.9338	6
2.136	122	45	2.1511	2.1370	122	42.0000	42.2915	11
1.915	131	2	1.9249	1.9063	131	47.2180	47.7071	54
1.797	402	20	1.8017	1.7894	402	50.6660	51.0398	5
1.794	420	30	1.7179	1.7758	420	53.3250	51.4568	4
1.633	511	2	1.6405	1.6170	511	56.0580	56.9451	43
1.559	004	6	1.5583	1.5774	004	59.3000	58.5142	13
1.555	422	12	1.5189	1.5475	422	61.0000	59.7565	6
1.389	042	10	1.3733	1.3847	042	68.3000	67.6568	10
1.271	404	2	1.2979	1.2764	404	72.8750	74.3062	4
1.178	215	4	1.1780	1.1891	215	81.7500	80.8308	4
1.101	044	2	1.1099	1.1023	044	87.9830	88.7468	10

Table 3 Crystal structure and parameters obtained with BC powder

Properties	Standard XRD data for $BaCeO_3$ powder (JCPDS no. 22–74)	Obtained XRD data for BCGO powder
Crystal structure	Orthorhombic	Orthorhombic
Unit cell lattice parameters (Å)	a = 8.779	a = 8.69065
	b = 6.214	b = 6.16463
	c = 6.236	c = 6.30943
Unit cell volume (Å^3)	340.1906	338.0254
Theoretical density (g/cc)	6.3533	6.3940
Crystallite size (nm)	-	11.52

$$0.3\ \mathrm{NaOH} \rightarrow 0.3\ \mathrm{Na^+_{(aq)}} + 0.3\ \mathrm{OH^-_{(aq)}},$$

$$0.05\ \mathrm{Ba(NO)_3} \rightarrow 0.05\ \mathrm{Ba^{2+}_{(aq)}} + 0.05\ \mathrm{NO_3{}^-_{(aq)}} 0.05\ \mathrm{Ce(NO_3)_3}\ .6H_2O_{(s)} \rightarrow 0.05\ \mathrm{Ce^{3+}_{(aq)}} + 0.15\ \mathrm{NO_3{}^-_{(aq)}} + 6H_2O_{(aq)},$$

$$0.05\ \mathrm{Ba^{2+}_{(aq)}} + 0.05\ \mathrm{Ce^{3+}_{(aq)}} + 0.3\ \mathrm{OH^-_{(aq)}} + x\ H_2O_{(aq)} \rightarrow 0.05\ \mathrm{Ba(OH)_2}\ .x\ H_2O_{(s)}\downarrow + 0.05\ \mathrm{Ce(OH)_4}\ .x\ H_2O_{(s)}\downarrow,$$

$$50^\circ C - 100^\circ C\ 0.05\ \mathrm{Ba(OH)_2}\ .x\ H_2O_{(s)} + 0.05\ \mathrm{Ce(OH)_4}\ .xH_2O_{(s)} \rightarrow 0.05\ \mathrm{Ba(OH)_{2(S)}} + 0.05\ \mathrm{Ce(OH)_{4(s)}} + x\ H_2O_{(g)}\uparrow,$$

$$600^\circ C\ 0.05\ \mathrm{Ba(OH)_{2(S)}} + 0.05\ \mathrm{Ce(OH)_{4(s)\ 3}} \rightarrow 0.05\ \mathrm{BaCeO_3} + x\ H_2O_{(g)}\uparrow$$

Reaction mechanism involved in the preparation of $BaCe_{0.9}Gd_{0.1}O_{3-\delta}$:

$$5.9\ \mathrm{NaOH} \rightarrow 5.9\ \mathrm{Na^+_{(aq)}} + 5.9\ \mathrm{OH^-_{(aq)}},$$

$$\mathrm{Ba(NO)_3} \rightarrow \mathrm{Ba^{2+}_{(aq)}} + \mathrm{NO_3{}^-_{(aq)}} 0.9\ \mathrm{Ce(NO_3)_3}\ .6H_2O_{(s)} \rightarrow 0.9\ \mathrm{Ce^{3+}_{(aq)}} + 2.7\ \mathrm{NO_3{}^-_{(aq)}} + 6H_2O_{(aq)},$$

$$0.1\ \mathrm{Gd(NO_3)_3} \rightarrow 0.1\ \mathrm{Gd^{3+}_{(aq)}} + 0.3\ \mathrm{NO_3{}^-_{(aq)}},$$

$$\mathrm{Ba^{2+}_{(aq)}} + 0.9\ \mathrm{Ce^{3+}_{(aq)}} + 0.1\ \mathrm{Gd^{3+}} + 5.9\ \mathrm{OH^-_{(aq)}} + x\ H_2O_{(aq)} \rightarrow \mathrm{Ba(OH)_2}\ .x\ H_2O_{(s)}\downarrow + 0.9\ \mathrm{Ce(OH)_4}\ .x\ H_2O_{(s)}\downarrow + 0.1\ \mathrm{Gd(OH)_3}\ .x\ H_2O_{(s)}\downarrow,$$

$$50^\circ C - 100^\circ C\ \mathrm{Ba(OH)_2}\ .x\ H_2O_{(s)} + 0.9\ \mathrm{Ce(OH)_4}\ .xH_2O_{(s)} + 0.1\ \mathrm{Gd(OH)_3}\ .x\ H_2O_{(s)} \rightarrow \mathrm{Ba(OH)_{2(S)}} + 0.9\ \mathrm{Ce(OH)_{4(s)}} + 0.1\ \mathrm{Gd(OH)_{3(s)}} + x\ H_2O_{(g)}\uparrow,$$

$$600^\circ C\ \mathrm{Ba(OH)_{2(S)}} + 0.9\ \mathrm{Ce(OH)_{4(s)}} + 0.1\ \mathrm{Gd(OH)_3} \rightarrow \mathrm{BaCe_{0.9}Gd_{0.1}O_{3-\delta}} + x\ H_2O_{(g)}\uparrow$$

Reaction mechanism involved in the preparation of $BaCe_{0.8}Sm_{0.2}O_{3-\delta}$:

Table 4 XRD data obtained with BCGO powder

Standard XRD data for orthorhombic $BaCeO_3$ powder (JCPDS no. 22–74)			Powder XRD data for $BaCe_{0.9}Gd_{0.1}O_{2-\delta}$					
d values (Å)	hkl values	I/I_o	d_{obs} (Å)	d_{cal} (Å)	hkl values	2θ values (obs)	2θ values (cal)	I/I_o (obs)
3.12	002	100	3.1675	3.1853	002	28.172	28.0114	100
2.659	112	2	2.7367	2.6969	112	32.722	33.2189	28
1.915	131	2	1.9288	1.9153	131	47.117	47.4683	56
1.633	511	2	1.6419	1.6423	511	56.007	55.9923	44
1.392	233	8	1.4017	1.4029	233	66.729	66.6676	4
1.389	042	10	1.3887	1.3913	042	67.437	67.2964	3

Table 5 Crystal structure and parameters obtained with BCGO powder

Properties	Standard XRD data for $BaCeO_3$ powder (JCPDS no. 22–74)	Obtained XRD data for BCGO powder
Crystal structure	Orthorhombic	Orthorhombic
Unit cell lattice parameters (Å)	a = 8.779	a = 8.83872
	b = 6.214	b = 6.18647
	c = 6.236	c = 6.37058
Unit cell volume ($Å^3$)	340.1906	348.3463
Theoretical density (g/cc)	6.3533	6.2219
Crystallite size (nm)	-	9.4525

$$5.8\ \mathrm{NaOH} \rightarrow 5.8\ \mathrm{Na^+_{(aq)}} + 5.8\ \mathrm{OH^-_{(aq)}},$$

$$\mathrm{Ba(NO)_3} \rightarrow \mathrm{Ba^{2+}_{(aq)}} + \mathrm{NO_3{}^-_{(aq)}} 0.8\ \mathrm{Ce(NO_3)_3}.6H_2O_{(s)} \rightarrow 0.8\ \mathrm{Ce^{3+}_{(aq)}} + 2.4\ \mathrm{NO_3{}^-_{(aq)}} + 6H_2O_{(aq)},$$

$$0.2\ \mathrm{Sm(NO_3)_3} \rightarrow 0.2\ \mathrm{Sm^{3+}_{(aq)}} + 0.6\ \mathrm{NO_3{}^-_{(aq)}},$$

$$\mathrm{Ba^{2+}_{(aq)}} + 0.8\ \mathrm{Ce^{3+}_{(aq)}} + 0.1\ \mathrm{Sm^{3+}} + 5.8\ \mathrm{OH^-_{(aq)}} + x\,H_2O_{(aq)} \rightarrow \mathrm{Ba(OH)_2}\ .x\,H_2O_{(s)}\downarrow + 0.8\ \mathrm{Ce(OH)_4}.x\,H_2O_{(s)}\downarrow + 0.2\ \mathrm{Sm(OH)_3}.x\,H_2O_{(s)}\downarrow,$$

$$50^{\circ}C\text{–}100^{\circ}C\quad \mathrm{Ba(OH)_2}\ .x\,H_2O_{(s)} + 0.8\ \mathrm{Ce(OH)_4}\ .xH_2O_{(s)} + 0.2\ \mathrm{Sm(OH)_3}\ .x\,H_2O_{(s)} \rightarrow \mathrm{Ba(OH)_{2(S)}} + 0.8\ \mathrm{Ce(OH)_{4(s)}} + 0.2\ \mathrm{Sm(OH)_{3(s)}} + x\,H_2O_{(g)}\uparrow,$$

$$600^{\circ}C\ \mathrm{Ba(OH)_{2(S)}} + 0.8\ \mathrm{Ce(OH)_{4(s)}} + 0.2\ \mathrm{Sm(OH)_3} \rightarrow \mathrm{BaCe_{0.9}Sm_{0.2}O_{3-\delta}} + x\,H_2O_{(g)}\uparrow$$

Thermal analysis of the precursor material was performed with SI EXSTAR 6000 TG/DTA 6300 instrument (Hitachi, Tokyo, Japan) between 25°C and 700°C in nitrogen atmosphere. The powder X-ray diffraction (XRD) studies were carried out using a Shimadzu XRD6000 X-ray diffractometer (Shimadzu, Kyoto, Japan) at a scan speed of 5°/min using CuKα radiation. The lattice parameters were calculated by least square fitting method using DOS computer programming. The theoretical density of the powders was calculated with the obtained XRD data. Energy-dispersive X-ray spectroscopy (EDAX) analysis was performed with a JEOL model JSM-6360 (JEOL Ltd., Tokyo, Japan) to find out the percentage of elements present in the samples. The crystallite sizes of the powder were calculated using Scherrer's formula. A Bruker IFS 66 V FTIR spectrometer (Bruker AXS, Madison, WI, USA) was employed to record the Fourier transform infrared (FTIR) spectra of doped $BaCeO_3$ powder in the range of 4,000 to 400 cm^{-1}. The crystallite sizes of the ceramic powders were calculated using Scherrer's formula. The particle size of the powder was measured with a Malvern particle size analyzer (Malvern Instruments, Worcestershire, UK) using triple-distilled water as medium. The surface morphology of the particles was studied using JEOL model JSM-6360 scanning electron microscope.

Results and discussion

Thermogravimetry/differential thermal analysis of precursor materials

The TGA/DTA spectra obtained with the precursor materials (($Ba(OH)_2$ + $Ce(OH)_4$ + $Gd(OH)_3$ + PVP) and ($Ba(OH)_2$ + $Ce(OH)_4$ + $Sm(OH)_3$ + PVP)) are indicated in Figures 2 and 3. The DTA peaks closely correspond

Table 6 XRD data obtained with BCSO powder

Standard XRD data for orthorhombic $BaCeO_3$ powder (JCPDS no. 22–74)			Powder XRD data for $BaCe_{0.8}Sm_{0.2}O_{2-\delta}$					
d values (Å)	hkl values	I/I_o	d_{obs} (Å)	d_{cal} (Å)	hkl values	2θ values (obs)	2θ values (cal)	I/I_o (obs)
3.12	002	100	3.1538	3.1496	002	28.297	28.3354	100
2.659	112	2	2.7281	2.6677	112	32.828	33.5928	31
1.915	131	2	1.9277	1.8870	131	47.145	48.2241	54
1.633	511	2	1.6422	1.6438	511	55.995	55.9362	45
1.559	004	6	1.5737	1.5748	004	58.663	58.6184	10
1.389	042	10	1.3614	1.3702	042	68.981	68.4745	9

Table 7 Crystal structure and parameters obtained with BCSO powder

Properties	Standard XRD data for $BaCeO_3$ powder (JCPDS no. 22–74)	Obtained XRD data for BCSO powder
Crystal structure	Orthorhombic	Orthorhombic
Unit cell lattice parameters (Å)	a = 8.779	a = 8.86793
	b = 6.214	b = 6.08696
	c = 6.236	c = 6.29920
Unit cell volume ($Å^3$)	340.1906	340.0228
Theoretical density (g/cc)	6.3533	6.3653
Crystallite size (nm)	-	9.6177

to the weight changes observed on the TGA curves. From Figure 2, the total weight loss at the temperature of 25°C to 700°C was found to be 10.0%. From the curve, it is understood that the weight loss begins to appear from the initial stage. The weight loss of about 3.6% is found at around 100°C, which is due to the removal of water molecule from the water sample. Then, the total weight loss of 5.7% is found at around 250°C, which is attributed to the removal of organics present in the sample. This is confirmed with an exothermic peak around 250°C in the DTA curve. The further weight loss present in the sample until 700°C is due to the decomposition of remaining carbon/nitrogen-based compounds from the sample.

From Figure 3, the total weight loss at the temperature of 25°C to 500°C was about 12%. This reduction in weight is attributed to the removal of water and other carbon and nitrogen oxides evolved from the sample during gradual heat treatment. From the curve, it is clear that the weight loss at 100°C is around 4.7%, which is attributed to the removal of water molecule from the sample. A strong exothermic peak found at around 258°C in the DTA curve indicates the start of the removal of carbon- and nitrogen-based compounds from the sample. At around 700°C, the weight loss is stable, which indicates the formation of phase-pure doped $BaCeO_3$.

Structural determination of doped $BaCeO_3$ particles by powder X-ray diffraction

It has been reported that the XRD patterns of rare-earth-oxide-doped $BaCeO_3$ is indexed to the orthorhombic crystal system with space group *Pnma* [10]. By using neutron diffraction measurements at high temperatures, Knight reported that crystal structure of $BaCeO_3$ at room temperature was orthorhombic distorted perovskite with space group of *Pnma* (no. 62) [11]. He also reported three types of structural phase transitions: from primitive orthorhombic perovskite to body-centered one with space group of *Imma* (no. 74), from the *Imma* to rhombohedrally distorted one with space group of *R3c* (no. 167), and from the *R3c* to cubic one with space group of *Pm3m* (no. 227) at 290°C, 400°C, and 900°C, respectively. Knight also investigated the structural phase transition of $BaCe_{1-x}M_xO_{3-\delta}$ by neutron diffraction measurements. Chen and Gulin synthesized $BaCe_{1-x}Gd_xO_{3-\delta}$ ($0.05 \le x \le 0.20$) by a microemulsion method and studied their structural properties. They reported that the structure of $BaCeO_3$ was found to be orthorhombic [12]. Gorbova et al. [13] have studied the structural and electrical properties of samarium-doped barium cerate ($BaCe_{1-x}Sm_xO_{3-\delta}$, with x = 0 to 0.2)

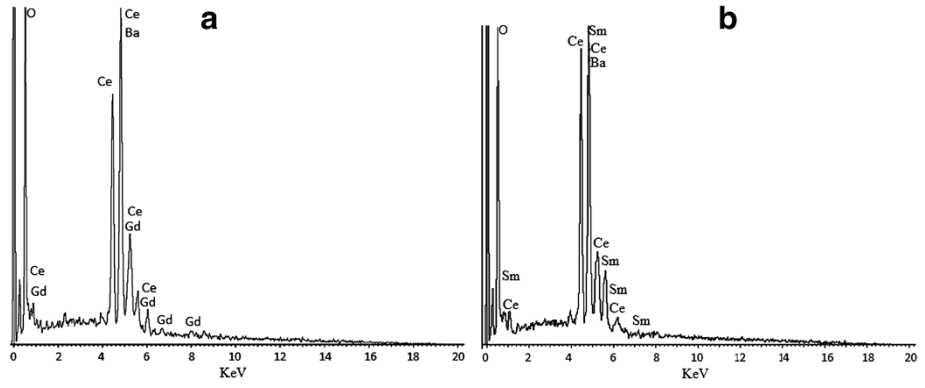

Figure 5 EDAX spectra obtained with calcined (a) BCGO and (b) BCSO powders prepared by chemical precipitation.

Table 8 Chemical composition data obtained with BCGO and BCSO powders by EDAX analysis

Sample	Weight % of elements
$BaCe_{0.9}Gd_{0.1}O_{3-\delta}$	Ba = 43.09
	Ce = 31.01
	Gd = 3.13
	O = 22.77
$BaCe_{0.8}Sm_{0.2}O_{2-\delta}$	Ba = 48.15
	Ce = 23.98
	Sm = 6.45
	O = 21.43

prepared by solid-state reaction method. They found that according to the XRD analysis at $0 \le x \le 0.2$, the formed continuous series of $BaCe_{1-x}Sm_xO_{3-\delta}$ solid solutions have the structure of cubic perovskite with orthorhombic distortions. Matskevich et al. [11] have studied the structural properties of $BaCe_{0.9}Ga_{0.1}O_{3-\delta}$, and they reported the structure as orthorhombic with unit cell parameters a = 6. 23413 Å, b = 6.21236 Å, and c = 8.77180 Å. The lattice parameter of Ba $(Ce_{0.8}Zr_{0.2})_{0.95}Yb_{0.05}O_{2.975}$ oxide prepared by Pechini method and calcined at 1,400°C was estimated and found to be a = 8.737 Å, b = 6.182 Å, and c = 6.197 Å (V = 334.713 Å^3) [14].

In this work, the structural properties of the parent $BaCeO_3$, $BaCe_{0.9}Gd_{0.1}O_{3-\delta}$, and $BaCe_{0.8}Sm_{0.2}O_{3-\delta}$ synthesized by chemical precipitation technique are investigated by XRD observation, which are demonstrated in Figure 4. The XRD patterns of the undoped and doped $BaCeO_3$ match with the standard data for $BaCeO_3$ (JCPDS card no. 22–74), indicating an orthorhombic crystal structure. In the XRD pattern of $BaCeO_3$, one additional peak was observed at 2θ = 23.8°, which may be due to the presence of impurity in the sample. However, in the doped $BaCeO_3$ sample, no other peak corresponding to any impurity was observed. The diffraction patterns of the $BaCe_{0.9}Gd_{0.1}O_{3-\delta}$ and $BaCe_{0.8}Sm_{0.2}O_{3-\delta}$ are similar to that of reported $BaCeO_3$ except for slight shifts in the diffraction angles. However, the presence of additional peaks in the parent $BaCeO_3$ matched well with the standard data reported in JCPDS card no. 22–74. The lattice parameters are calculated from 2θ values in the X-ray diffraction patterns. The powder XRD data obtained with $BaCeO_3$, $BaCe_{0.9}Gd_{0.1}O_{3-\delta}$, and $BaCe_{0.8}Sm_{0.2}O_{3-\delta}$ are reported in Tables 2, 3, 4, 5, 6, and 7. The unit cell volume, crystallite size, and theoretical density values are calculated for these samples, and the values were found to be similar to each other. The theoretical density calculated from the XRD data for the $BaCeO_3$ powder was reported as 5.96 g/cm^3. Also, it is reported that the crystallite size calculated for $BaCeO_3$ powder was lower than the actual grain size measured by sophisticated techniques like scanning electron microscopy (SEM) [15]. The reported data on the crystallographic properties for $BaCeO_3$ agree with the parent and doped $BaCeO_3$ reported in this paper.

Chemical composition of the of doped $BaCeO_3$ powders

The EDAX spectra obtained with BCGO and BCSO powders are reported in Figure 5. The chemical composition data derived for the samples from the EDAX

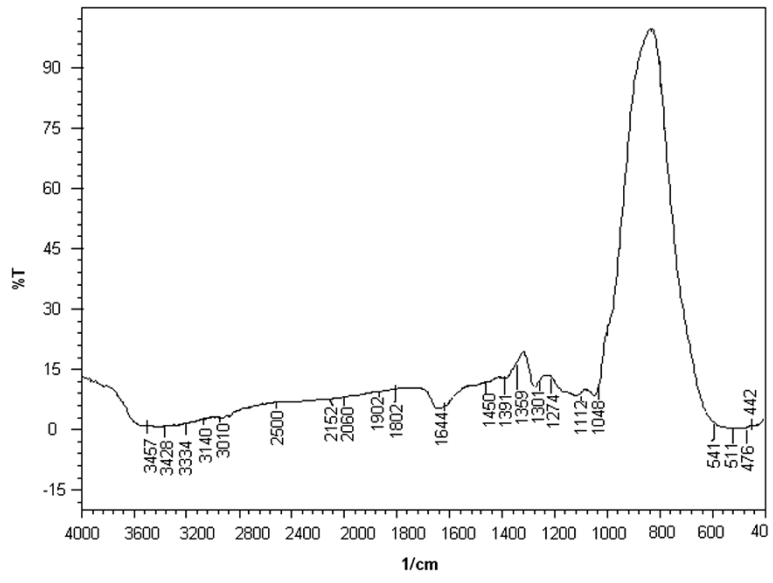

Figure 6 FTIR spectrum obtained with calcined BCGO powder prepared by chemical precipitation method.

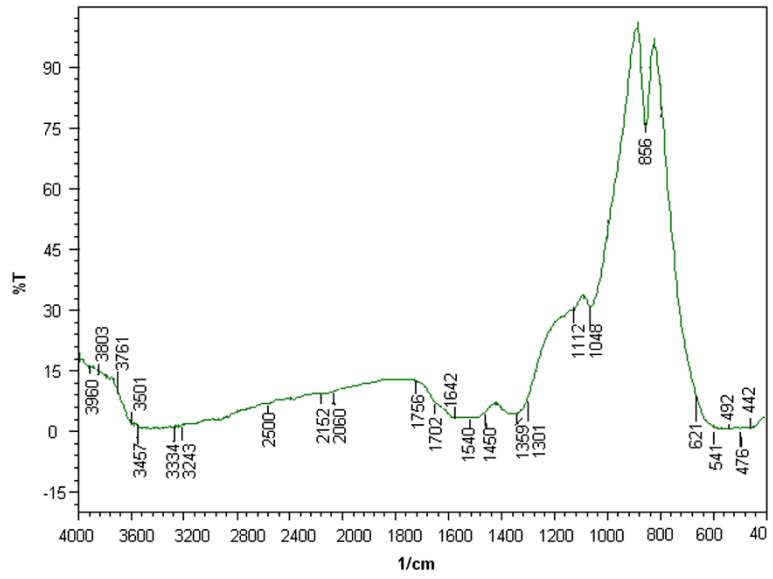

Figure 7 FTIR spectrum obtained with calcined BCSO powder prepared by chemical precipitation method.

analysis is indicated in Table 8. From the data, it was found that the elements were present as per the requirement.

FTIR spectroscopic studies of doped $BaCeO_3$ powders

Figures 6 and 7 show the FTIR spectra obtained with BCGO and BCSO powders prepared by chemical precipitation method. FTIR measurements were done using KBr method at room temperature. The wide absorption bands that appeared at 3,428 cm^{-1} in BCGO and 3,457 cm^{-1} in BCSO are attributed to the stretching vibration of water H-O bond (moisture) [16]. According to standard IR spectra, peaks that appeared at 1,391 and 511 cm^{-1} in BCGO and 1,359 and 541 cm^{-1} in BCSO, as well as the shoulder peaks that appeared around 1,500 to 1,700 cm^{-1} in both samples, are attributed to the Ce-O in the sample as reported [17]. Also, the bands that appeared at around 2,500 cm^{-1} in both samples are attributed to the presence of CO_2 in the sample [18]. The bands in the region 1,000 to 650 cm^{-1} have been assigned to the stretching modes, and the region 650 to 450 cm^{-1} contains bridging stretching modes in both samples [19].

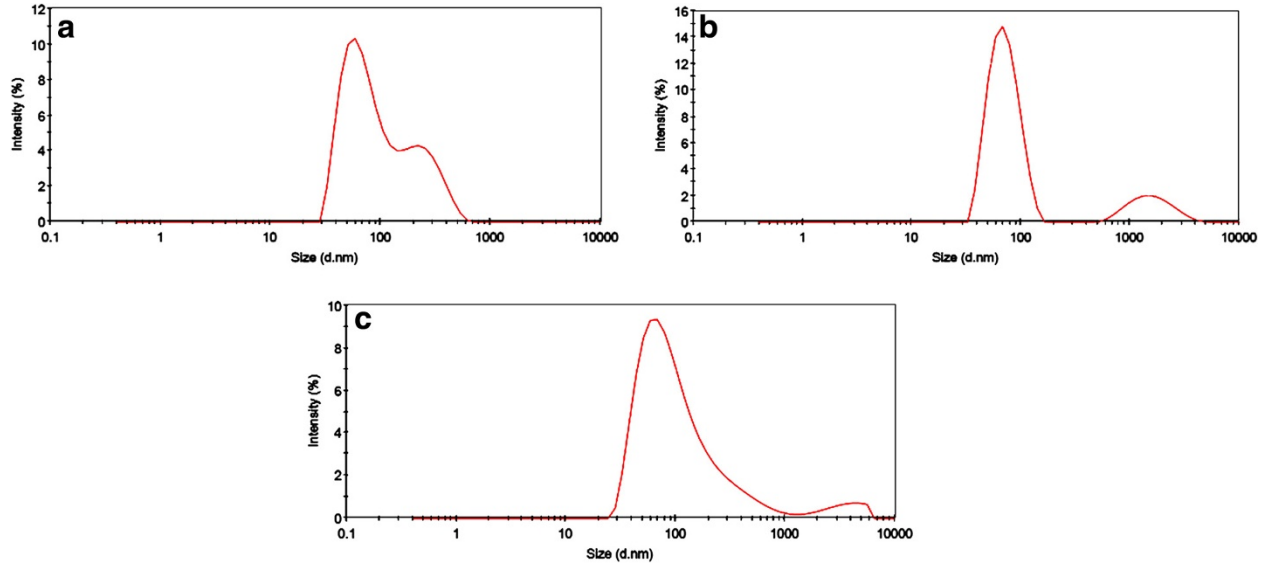

Figure 8 Particle size distribution patterns (based on intensity) obtained with BCGO powder prepared by chemical precipitation. For the different trials (**a**, **b**, **c**) carried out for particle size analysis.

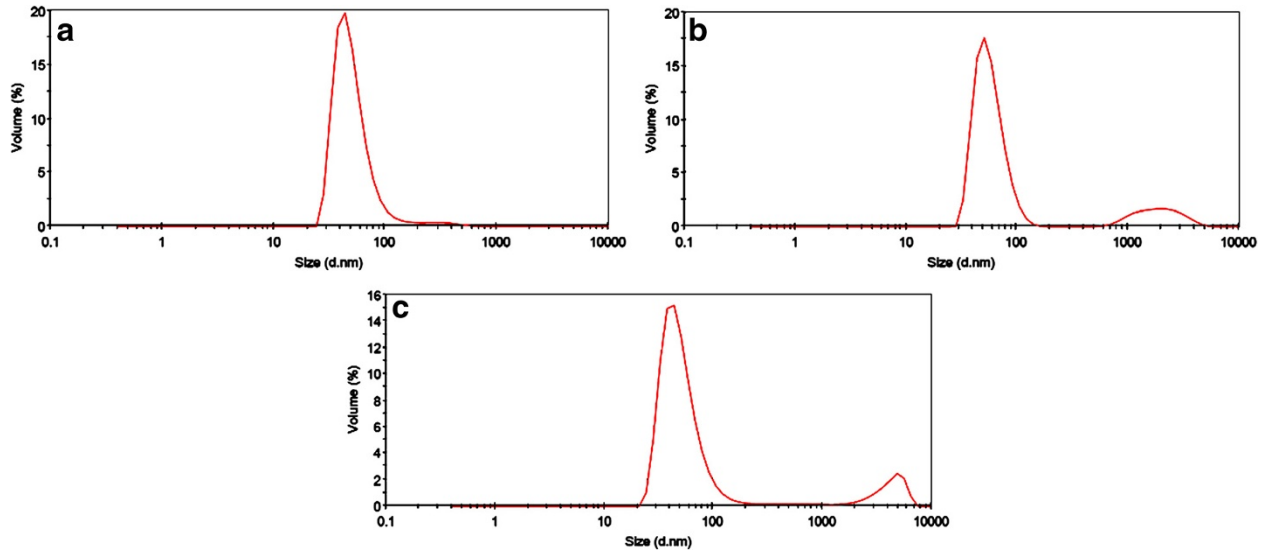

Figure 9 Particle size distribution patterns (based on volume) obtained with BCGO powder prepared by chemical precipitation. For the different trials (**a**, **b**, **c**) carried out for particle size analysis.

Particulate properties obtained with BCGO/BCSO powders

The prepared doped barium cerate particles were subjected to particle size measurements using a Malvern particle size analyzer with triple-distilled water as medium. For all the measurement, 0.20 g of sample was sonicated in 200 ml of triple-distilled water for about 5 min, and after that, the sample was subjected to particle size analysis. The particle size distribution curves obtained with BCGO and BCSO samples prepared by chemical precipitation method are shown in Figures 8, 9, 10 and 11, respectively. The particle characteristics are indicated in Tables 9, 10, 11, and 12, respectively. From Figures 10 and 11 and the particle characteristic data (Tables 11 and 12), it was understood that the average particle size of BCSO powder prepared by chemical precipitation method is found to be around the range of 110.4 to 132.1 nm, which is higher than the particle size data obtained for other samples. The presence of higher

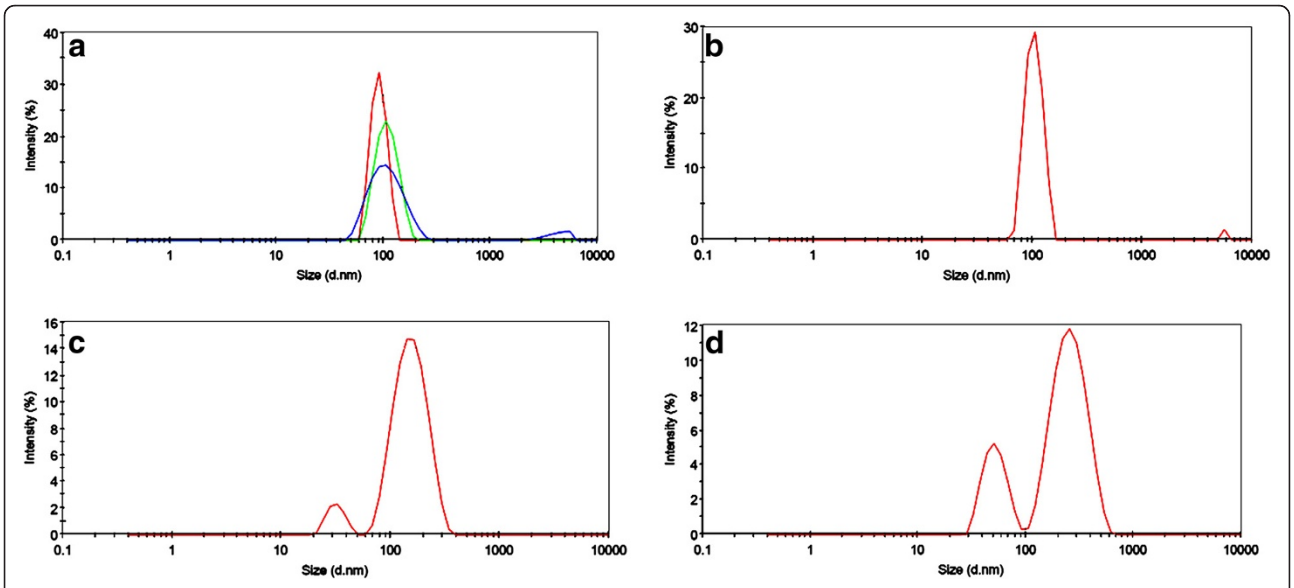

Figure 10 Particle size distribution patterns (based on intensity) obtained with BCSO powder prepared by chemical precipitation. For the different trials (**a**, **b**, **c**, **d**) carried out for particle size analysis. The colored lines indicate the measurement recorded details.

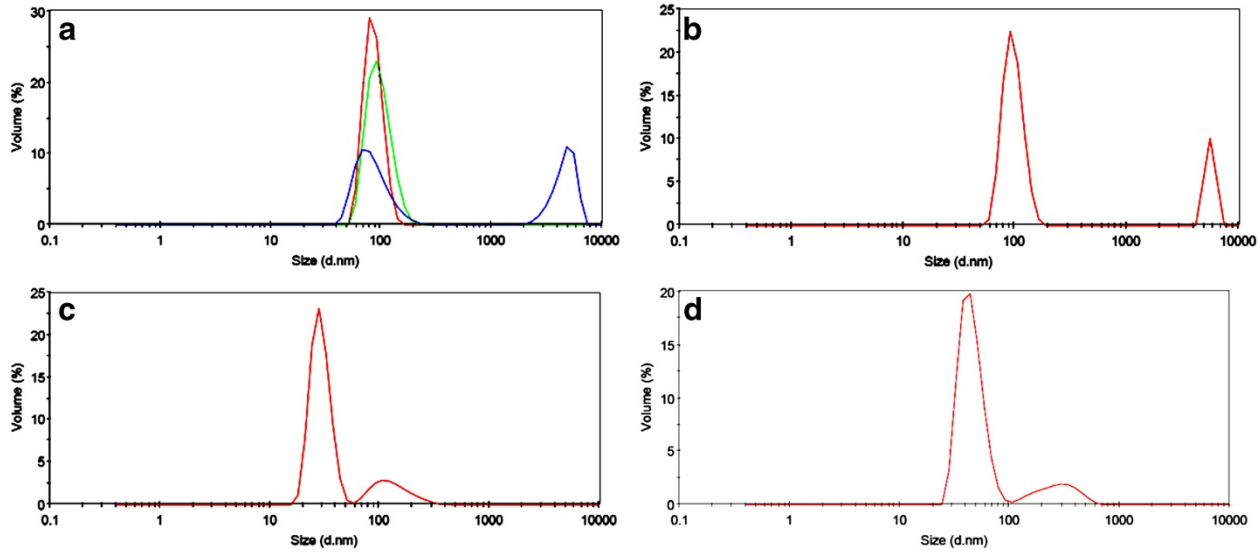

Figure 11 Particle size distribution patterns (based on volume) obtained with BCSO powder prepared by chemical precipitation. For the different trials (**a**, **b**, **c**, **d**) carried out for particle size analysis. The colored lines indicate the measurement recorded details.

Table 9 Particle characteristic data (based on intensity) obtained with BCGO powder prepared by chemical precipitation method

Trial	Peak 1		Peak 2		Peak 3		Average particle size (nm)
	Intensity (%)	Diameter (nm)	Intensity (%)	Diameter (nm)	Intensity (%)	Diameter (nm)	
1	70	71.71	30	79.15	-	-	79.15
2	83.7	72.20	16.3	77.54	-	-	77.54
3	86.5	52.65	1.8	651.4	11.7	4186	82.49

Table 10 Particle characteristic data (based on volume) obtained with BCGO powder prepared by chemical precipitation method (with 2 ml PVP)

Trial	Peak 1		Peak 2		Average particle size (nm)
	Volume (%)	Diameter (nm)	Volume (%)	Diameter (nm)	
1	97.9	52.12	2.1	334.6	79.15
2	85.0	57.51	15	1999	77.54
3	94.7	130.2	5.3	3463	82.49

Table 11 Particle characteristic data (based on intensity) obtained with BCSO powder prepared by chemical precipitation method

Trial	Peak 1		Peak 2		Average particle size (nm)
	Intensity (%)	Diameter (nm)	Intensity (%)	Diameter (nm)	
1	92.9	111.7	7.1	4276	110.4
2	98.6	104.2	1.4	5560	130.6
3	92.0	159.2	8.0	31.94	117.2
4	76.6	266	23.4	52.74	132.1

Table 12 Particle characteristic data (based on volume) obtained with BCSO powder prepared by chemical precipitation method

Trial	Peak 1		Peak 2		Average particle size (nm)
	Volume (%)	Diameter (nm)	Volume (%)	Diameter (nm)	
1	58.5	86.34	41.5	4662	110.4
2	79.8	97.42	20.2	5590	130.6
3	18.8	134.9	81.2	29.36	117.2
4	14.8	285.7	85.2	45.59	132.1

particle size may be due to the agglomeration of particles at high-temperature treatment [20].

SEM studies of doped $BaCeO_3$ powders

The SEM photographs obtained with BCGO and BCSO are shown in Figure 12. From the micrographs (Figure 12a,b), it was noticed that the surface of Gd-doped $BaCeO_3$ was not smooth. Bigger grains were also seen. The grain size varied from the lower side to higher side. The presence of bigger particles in the sample ($BaCe_{0.9}Gd_{0.1}O_{2-\delta}$) is due to the combination of few particles together at high temperature. The average grain size of $BaCe_{0.9}Gd_{0.1}O_{2-\delta}$ was found to be around 70 nm. From Figure 12c,d, it was understood that different size of particles were present in the $BaCe_{0.8}Sm_{0.2}O_{2-\delta}$ powder. The surface was rough. The grain size was found to be in the range of 50 to 70 nm in $BaCe_{0.8}Sm_{0.2}O_{2-\delta}$ powder. The presence of large particles (>100 nm) may be due to the agglomeration of particles during high-temperature treatment.

Experimental

This research paper describes the preparation of $BaCe_{1-x}M_xO_{3-\delta}$ (where M = Gd or Sm and x = 0, 0.10, or 0.20) by a simple low-temperature chemical precipitation method. The precursor materials used in this research work were barium nitrate, cerium nitrate, and gadolinium nitrate/samarium nitrate (as basic materials); sodium hydroxide (as a precipitator material); and polyvinyl pyrrolidone (as surfactant). In a

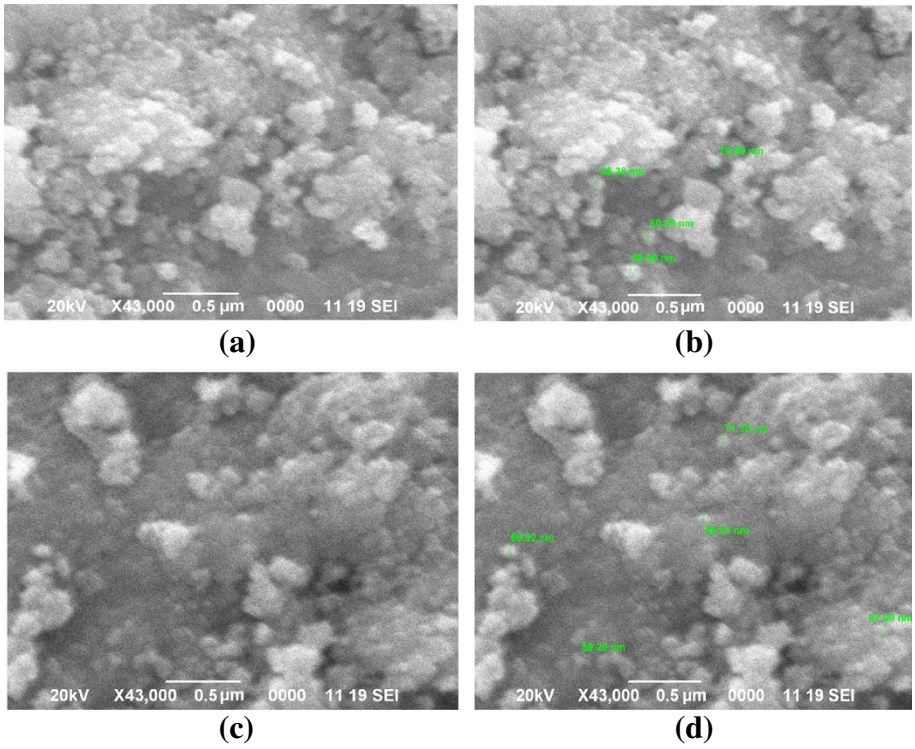

Figure 12 SEM photographs obtained with calcined (a, b) BCGO and (c, d) BCSO powder.

typical experiment, the aqueous solution containing Ba^{2+}, Ce^{3+}, and Gd^{3+}/Sm^{3+} ions was mixed with the solution of alkali in a magnetic stirrer, and then the required percentage of surfactant was added. The formed hydroxides of Ba, Ce, and Gd/Sm were washed with water and ethyl alcohol, dried at 50°C to 100°C for 24 h, and finally, heat-treated at 300°C, 450°C, and 600°C for 2 h each to get phase-pure products. Suitable reaction mechanisms were proposed for the preparation of $BaCeO_3$-based materials.

Conclusions

The preparation of phase-pure BCGO and BCSO nanoparticles using barium nitrate, cerium nitrate hexahydrate, Gd_2O_3, Sm_2O_3, nitric acid, sodium hydroxide, and surfactant (PVP) by simple wet chemical method (chemical precipitation method) is dealt with. The TGA/DTA data revealed the removal of moisture and other organics from the precursor materials. Also, the TGA/DTA data helped to find out the suitable calcination temperature to prepare phase-pure compound. The powder XRD data obtained with parent and doped $BaCeO_3$ powder is in good agreement with the standard reported JCPDS data. The crystalline structure of $BaCeO_3$ is orthorhombic. The EDAX data confirmed the presence of required elements in both samples. From the FTIR data, it is understood that the characteristic peak of Ce-O is present in both samples. The particulate properties of both samples suggest that the particles are present in nanometer range. The presence of nanosized particles in both samples is also confirmed with SEM data. After measuring the protonic conductivity of doped $BaCeO_3$ nanomaterials, these materials may be utilized for application in SOFCs as electrolyte materials.

Competing interests

The authors declare that they have no competing interests.

Authors' contributions

ASN designed the experimental methodology and drafted the manuscript. JJK and DR carried out the experiments. All authors read and approved the final manuscript.

Authors' information

JJK and DR are research scholars at the Department of Chemistry, Karunya University, Coimbatore, India. They are working in the synthesis and characterization of novel materials applicable for low-temperature solid oxide fuel cells.

ASN is working as an associate professor and admissions officer at the Department of Chemistry, Karunya University, Coimbatore, India. He is working in the field of nanoparticles for application in electrochemical power sources since 1996. At present, four research scholars are working for their PhD degree under his guidance.

Acknowledgments

ASN thanks Karunya University for promoting high-temperature fuel cell research activity. Also, he thanks Dr. P. E. Jagadeesh Babu, NITK, Surathkal, India, for his help in the TG/DTA measurements.

Received: 19 September 2012 Accepted: 2 February 2013
Published: 26 February 2013

References

1. Kreuer KD (1997) Solid State Ionics 97:1
2. Yan R, Wang Q, Chen G, Huang W, Xie K (2009) Ionics 15:749
3. Tao Z, Zhu Z, Wang H, Liu W (2010) J Power Sources 195:3481
4. Wu J, Webb SM, Brennan S, Haile SM (2005) J App Phy 97:054101
5. Takeuchi K, Loong C-K, Richardson JW, Jr, Guan J, Dorris SE, Balachandran U (2000) Solid State Ionics 138:63
6. Ouzaouit K, Benlhachemi A, Benyaich H, Dallas JP, Villain S, Musso JA, Gavarri JR (2006) J Morocann Condensed Mater 7:94
7. Iwahara H, Esaka T, Uchida H, Maeda N (1981) Solid State Ionics 3&4:359
8. Bonanos N, Ellis B, Knight KS, Mahmood M (1989) Solid State Ionics 35:179
9. Zhen MH, Chen X (1994) Solid State Ionics 70&71:595
10. Matskevich NI, Chupahina TI, Bazuevsolutions GV, Kuznetsov FA (2005) New phases in the Ba–Ce(M)–O systems (M = Ga, In)
11. Knight KS (2001) Solid State Ionics 145:275
12. Chen C, Ma G (2009) J Alloys Compd 485:69
13. Gorbova E, Maragou V, Medvedev D, Demin A, Tsiakaras P (2008) J Power Sources 181:207
14. Osman N, Talib IA, Hamid HA (2009) Sains Malaysiana 38:401
15. Paul Inge D (2006) Synthesis and characterization of ionic conductors based on ZrO_2, $BaZrO_3$ and $SrCeO_3$ and preparation of $LaFeO_3$ and $LaCoO_3$ thin films. Doctoral thesis, Norwegian University of Science and Technology
16. Chao X, Junwu Z, Yang Xujie L, Lude WX (2008) J Rare Earths 26:51
17. Sadtler Research Laboratories (1965) Inorganics IR Grating Spectra. Sadtler Research Laboratories Inc, Philadelphia
18. Tas AC, Majewski PJ, Aldinger F (2000) J Am Ceram Soc 83:2954
19. Subramanya Herle P, Hegde MS, Subbanna GN (1997) J Mater Chem 7:2121
20. Rajiv Gandhi R, Suresh J, Gowri S, Selvam S, Sundrarajan M (2012) Adv Sci Lett 16:244

doi:10.1186/2228-5547-4-18
Cite this article as: Ketzial *et al.*: Low-temperature preparation and physical characterization of doped $BaCeO_3$ nanoparticles by chemical precipitation. *International Journal of Industrial Chemistry* 2013 **4**:18.